Ionospheric disturbances detected by GPS total electron content observation after the 2011 off the Pacific coast of Tohoku Earthquake

T. Tsugawa[1], A. Saito[2], Y. Otsuka[3], M. Nishioka[3], T. Maruyama[1], H. Kato[1], T. Nagatsuma[1], and K. T. Murata[1]

[1]*National Institute of Information and Communications Technology, Japan*
[2]*Department of Geophysics, Graduate School of Science, Kyoto University, Japan*
[3]*Solar-Terrestrial Environment Laboratory, Nagoya University, Japan*

(Received April 9, 2011; Revised June 21, 2011; Accepted June 22, 2011; Online published September 27, 2011)

All the details of ionospheric disturbances following the 2011 Tohoku Earthquake were first revealed by the high-resolution GPS total electron content observation in Japan. The initial ionospheric disturbance appeared as sudden depletions following small impulsive TEC enhancements ∼7 minutes after the earthquake onset, near the epicenter. Then, concentric waves appeared to propagate in the radial direction with a velocity of 138–3,457 m/s. Zonally-extended enhancements of the TEC also appeared in the west of Japan. In the vicinity of the epicenter, short-period oscillations with a period of ∼4 minutes were observed. This paper focuses on the concentric waves. The concentric pattern indicates that they had a point source. The center of these structures, termed the "ionospheric epicenter", was located about 170 km from the epicenter in the southeast direction. According to the propagation characteristics, these concentric waves could be caused by atmospheric waves classified into three types: acoustic waves generated from a propagating Rayleigh wave, acoustic waves from the ionospheric epicenter, and atmospheric gravity waves from the ionospheric epicenter. The amplitude of the concentric waves was not uniform and was dependent on the azimuth of their propagation direction, which could not be explained by previously-proposed theory.
Key words: Ionosphere, earthquake, tsunami, GPS, TEC, Japan.

1. Introduction

Various kinds of ionospheric disturbances following strong earthquakes have been studied for several decades (e.g., Davies and Baker, 1965). The vertical crustal movement during an earthquake causes the displacement of the atmosphere on the Earth's surface and excites atmospheric waves which propagate up to the thermosphere. They modulate the ionospheric plasma density through ion-neutral collisions. Two-dimensional ionospheric total electron content (TEC) observations using a dense GPS receiver network have recently been employed to examine ionospheric disturbances induced by earthquakes (Ducic *et al*., 2003; Liu *et al*., 2010) and tsunamis (Artru *et al*., 2005). Heki and Ping (2005) revealed circular TEC structures propagating from the epicenter after earthquakes off the Pacific coast of Japan. Although these previous studies revealed some aspects of ionospheric disturbances following earthquakes, there has been no observation of all the details of post-seismic ionospheric disturbances including their commencement near the epicenter and their evolution in a wider area.

Various ionospheric disturbances were observed after the 2011 off the Pacific coast of Tohoku Earthquake by high-resolution GPS-TEC observation in Japan. This paper and accompanying papers (Chen *et al*., 2011; Maruyama *et al*., 2011; Matsumura *et al*., 2011; Saito *et al*., 2011) report all the details of the commencement and evolution of ionospheric disturbances following this earthquake. The ins and outs of post-seismic ionospheric disturbances were first observed by a high-resolution two-dimensional GPS-TEC observation. The concentric ionospheric wave trains following earthquakes were also observed for the first time. In this paper, we will present an overview of all the ionospheric disturbances and clarify the characteristics of the concentric ionospheric disturbances propagating away from the epicenter. Saito *et al*. (2011) discussed the ionospheric variations in the vicinity of the epicenter. The long-distance propagation of ionospheric waves are discussed by Chen *et al*. (2011). Maruyama *et al*. (2011) discussed the vertical structure of the ionospheric variations based on ionosonde observations. Matsumura *et al*. (2011) studied the atmospheric waves by numerical simulations.

2. Data

We used the data of GEONET, a dense GPS receiver network operated by the Geospatial Information Authority of Japan. TEC, the integrated electron density along the entire line-of-sight (LOS) between receiver and satellite, was derived from the pseudo-ranges and phases of the dual-frequency GPS signals (Saito *et al*., 1998). The absolute TEC values were derived applying a technique in which a weighted-least-square fitting is used to determine unknown instrumental biases, assuming that the hourly TEC average

doi:10.5047/eps.2011.06.035

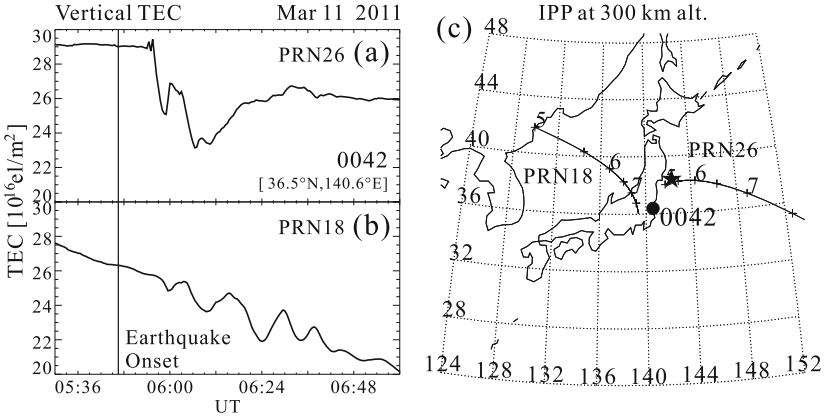

Fig. 1. Vertical TEC observed by the "0042" station from 05:30 UT to 07:00 UT (14:30–16:00 JST) on March 11, 2011, with the signal from (a) the PRN26 satellite and (b) the PRN18 satellite. (c) The location of "0042" station (dot) and ionospheric pierce points (IPP) of line-of-sight (LOS) for the PRN26 and the RPN18 satellite-receiver pairs (curves). The digits represent the corresponding UT hours. The star mark represents the location of the epicenter.

is uniform within the area covered by a given GPS receiver (Otsuka *et al.*, 2002).

3. Observations

A moment magnitude 9.0 earthquake struck off the Pacific coast of Japan at 05:46:23 UT on March 11, 2011 (US Geological Survey, 2011). The earthquake was named "the 2011 off the Pacific coast of Tohoku Earthquake" (the 2011 Tohoku Earthquake) by the Japan Meteorological Agency. The epicenter of this earthquake was (38.322°N, 142.369°E) in latitude and longitude.

Figures 1(a) and (b) show the absolute vertical TEC observed by the "0042" GPS station from 05:30 UT to 07:00 UT on March 11, 2011, with signals from the PRN26 and the PRN18 satellites, respectively, Fig. 1(c) shows the ionospheric pierce points (IPP) of line-of-sight (LOS) for the PRN26 and RPN18 satellite-receiver pairs. The digits represent the corresponding UT hours. The IPP for the PRN26 satellite was located in the vicinity of the epicenter at the earthquake onset. As shown in Fig. 1(a), the vertical TEC for the PRN26 satellite was an almost constant value of ∼29 TEC units until about seven minutes after the earthquake onset. One TEC unit (TECU) is 10^{16} m^{-2}. Around 05:54 UT, the TEC data showed two impulsive enhancements with amplitudes of 0.5–1.0 TECU. After the impulsive enhancements, TEC showed sudden depletions with perturbations at 05:56 UT and reached a minimum value of ∼23 TECU at 06:07 UT. The amplitude of the total TEC depletion was ∼6 TECU, 20% of the TEC before the depletions. In Fig. 1(b), the TEC perturbations whose amplitudes of 1–2 TECU were seen in the TEC data for the PRN18 satellite from 06:00 UT to 07:00 UT. During this period, the IPP for the PRN18 satellite moved southeastward from 39°N to 37°N and from 137°E to 139°E. It is noted that the initial TEC variation was negative. Any remarkable impulsive enhancements and sudden depletions were not seen, in contrast with those for the PRN26 satellite.

Two-dimensional maps of the detrended TEC from 05:50 UT and 07:25 UT on March 11, 2011, are shown in Fig. 2. The detrended TEC was derived by subtracting a 10-minute running average of the data for each LOS. The elevation mask of the LOS is 25°. The size of each pixel of Fig. 2 is 0.15°×0.15° in latitude and longitude. The detrended TEC value for each pixel is an average of data for all LOS which crossed the pixel at 300 km altitude. The data in each epoch is smoothed spatially with the running average of 3×3 pixel (0.45°×0.45°) in latitude and longitude. Figures 2(a–d), (d–f), and (f–h) show the time sequence of maps with a 5, 10, 30-minute interval, respectively. The color contour indicates −0.40 to 0.20 TECU. The epicenter is represented by star marks. A movie of Fig. 2 with a 30-second resolution is available at the NICT website (http://www.seg.nict.go.jp/2011TohokuEarthquake/).

The detrended TEC map at 05:50 UT in Fig. 2(a), about four minutes after the earthquake onset, indicates that any remarkable TEC variations were not observed over Japan. At 05:55 UT in Fig. 2(b), enhancements of the detrended TEC were observed in the vicinity of the epicenter. It is noted that the trend of the vertical TEC obtained with a 10-minute running average decreases (increases) within five minutes before the sudden depletion (enhancement) in the vertical TEC. The detrended TEC derived by subtracting this trend from the vertical TEC could show a virtual enhancement (depletion) during this period. Considering the time sequence of the vertical TEC in Fig. 1(a) and the characteristics of this detrended technique, the enhancements of the detrended TEC would correspond to the sudden depletions in the vertical TEC. The center of these enhancements (represented by cross marks in Fig. 2) was estimated to be around 37.5°N of latitude and 144.0°E of longitude. We termed this center the "ionospheric epicenter". The ionospheric epicenter was about 170 km distance from the epicenter in the southeast direction.

As shown in 5-minute interval maps of Figs. 2(c–d), large-scale waves with circular wavefronts propagated in the radial direction with a velocity of 3,457 m/s. These waves first produced TEC depletions corresponding to the negative TEC variations around 06:00 UT in Fig. 1(b). These large-scale circular waves had two negative peaks and a horizontal wavelength of more than 500 km. The center of these circular wave structures was almost the same as the ionospheric epicenter. In addition to these circular

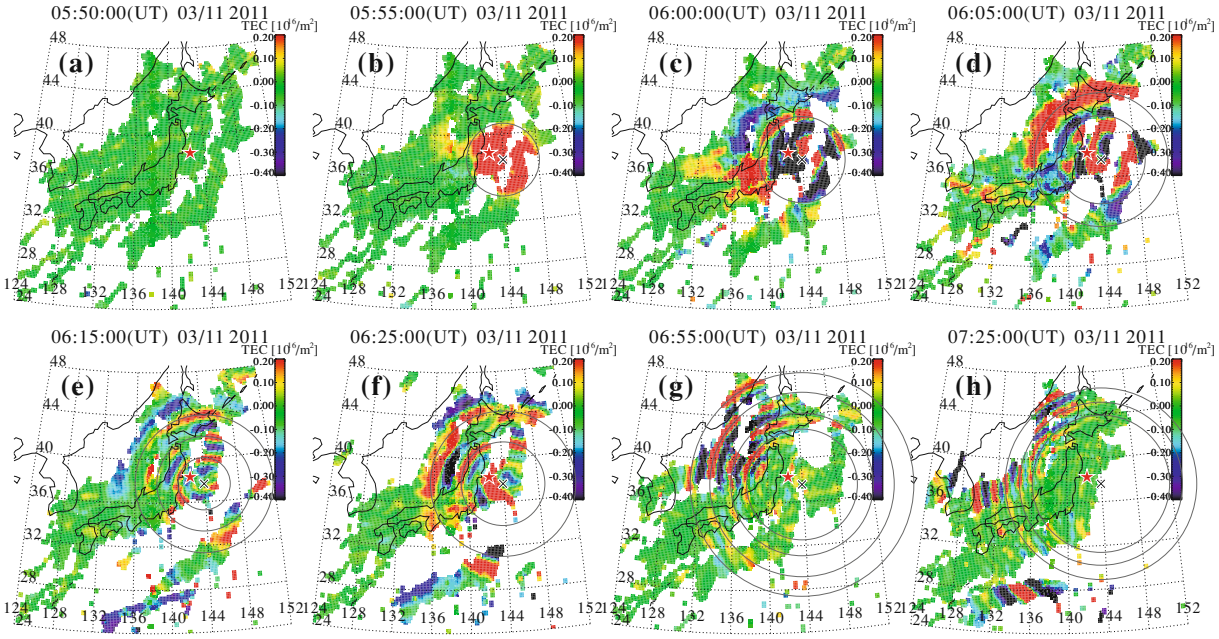

Fig. 2. Two-dimensional maps of the detrended TEC from 05:50 UT to 07:25 UT on March 11, 2011. The interval of figures (a–d), (d–f), and (f–h) is 5, 10, 30 minutes, respectively. The star and cross marks represent the epicenter and the ionospheric epicenter, respectively. Gray circles represent concentric circles with the ionospheric epicenter. A movie of the detrended TEC maps with 30-second resolution is available at the NICT website (http://www.seg.nict.go.jp/2011TohokuEarthquake/).

waves, zonally-extended enhancements of TEC appeared at 06:00 UT in 36–37°N of latitude and 130–140°E of longitude as shown in Fig. 2(c). This structure traveled in the southwest direction.

After the propagation of the first large-scale circular waves, medium-scale concentric waves with a wavelength of 200–300 km appeared almost all over Japan as shown in Figs. 2(f–h). The center of these concentric waves was also almost the same as the ionospheric epicenter. They propagated in a radial direction with a slower propagation velocity than the large-scale circular waves. They appeared until past 08:00 UT in the western part of Japan.

Figure 3 shows a time-longitude cross-section of the detrended TEC from 05:00 UT to 09:00 UT at 37.5°N, the same latitude as the ionospheric epicenter. The color contour in Fig. 3 is the same as Fig. 2. Fast westward propagations of two peaks appeared from 06:00 UT to 06:15 UT and from 130°E to 136°E. These TEC peaks correspond to the large-scale circular waves as shown in Figs. 2(c–e). From the evolutions of these TEC peaks represented by white dotted lines in Fig. 3, the propagation velocity was estimated to be 3,457 m/s and 783 m/s for the first and second large-scale waves, respectively. The amplitudes of the first and second TEC peaks decreased as they traveled westward and almost disappeared around 130°E and 132°E, respectively.

After around 06:15 UT, relatively slow westward propagations of TEC peaks appeared in the west from ∼140°E of longitude. These TEC peaks correspond to the medium-scale concentric waves as shown in Figs. 2(f–h). The first TEC peak of the medium-scale wave appeared around 06:30 UT at 135°E of longitude and propagated westward with a propagation velocity of 423 m/s. We identified several TEC peaks which are represented by black dotted lines with their propagation velocities in Fig. 3. These medium-

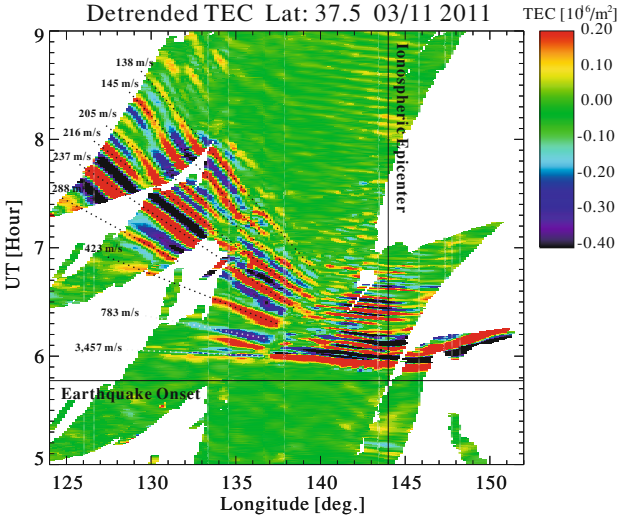

Fig. 3. Time-longitude cross-section of the detrended TEC with a 10-minute window along 37.5°N latitude from 124°E to 152°E from 05:00 UT to 09:00 UT. The color contour is the same as Fig. 2.

scale waves with longer wavelengths and larger propagation velocities appeared earlier in the western part of Japan. For example, around 130–133°E of longitude, waves with a velocity of 288 m/s and 145 m/s and wavelengths of 250 km and 130 km appeared at 07:00 UT and 08:00 UT, respectively. In contrast to the large-scale waves, these medium-scale waves were not so dissipated and propagated at least for a distance greater than 1,500 km from the ionospheric epicenter. They appeared in the western part of Japan until around 09:00 UT.

In addition to the concentric waves, the short-period oscillation with a period of about four minutes was observed

in the vicinity of the epicenter rather than the ionospheric epicenter after around 06:00 UT. Although the amplitude of this TEC oscillation decreased with time, it was observed for 3 hours or more.

4. Summary and Discussion

The high-resolution GPS-TEC observation in Japan was the first to reveal all the details of the commencement and evolution of ionospheric disturbances after the 2011 off the Pacific coast of Tohoku Earthquake. The remarkable ionospheric disturbances are summarized as follows:

(I) Sudden TEC depletions following small impulsive TEC enhancements around 05:54 UT, about seven minutes after the earthquake onset, appeared in the vicinity of the ionospheric epicenter.
(II) Zonally-extended enhancements in the detrended TEC appeared in the west of Japan at 06:00 UT and traveled in the southwest direction.
(III) Large-scale circular waves with two negative peaks, a large propagation velocity (3,457 m/s and 783 m/s), and strong dissipation (travelling distance is about 1,000 km) propagated in a radial direction from 06:00 UT to 06:15 UT.
(IV) Medium-scale concentric waves with a slower propagation velocity (138–423 m/s) and less dissipation propagated in a radial direction following the large-scale waves after 06:15 UT.
(V) Short-period oscillations appeared in the vicinity of the epicenter after 06:00 UT and continued for 3 hours or more.

As for the sudden TEC depletions (I), similar phenomena were observed after the 2010 Chile earthquake (Nishioka *et al*., 2011). Their mechanism, however, has not yet been clarified. The sudden TEC depletions in this event were investigated in detail by Saito *et al*. (2011). Chen *et al*. (2011) studied the detail characteristics of the zonally-extended TEC structures (II) which were also observed in Taiwan more than 2,500 km distance from the ionospheric epicenter in the southwest direction. The short-period oscillations in the vicinity of the epicenter (V) were investigated based on the GPS-TEC observations (Saito *et al*., 2011) and numerical simulations (Matsumura *et al*., 2011). They are explained by the acoustic resonance between the ground surface and the lower thermosphere. In this paper, we focus on the large- and medium-scale concentric waves (III, IV).

Similar TEC disturbances such as the large-scale circular waves (III) have been previously reported after earthquakes off the Pacific coast of Japan (Heki and Ping, 2005), the 2004 Sumatra earthquake (Otsuka *et al*., 2006), and the 2010 Chile earthquake (Nishioka *et al*., 2011). The propagation velocity of 3,457 m/s for the first peak is consistent with the velocity of a Rayleigh wave which is one type of surface wave produced during earthquakes (Oliver, 1962). It experiences less attenuation and propagates over several hundred kilometers. We speculate that the first peak of the large-scale circular wave was related to a Rayleigh wave propagating from the ionospheric epicenter. Since the velocity of a Rayleigh wave is much larger than the acoustic velocity, the acoustic wave launched by the propagating Rayleigh wave can reach the ionospheric altitude earlier than that launched by vertical displacement of the air above the sea surface at the ionospheric epicenter. The first peak of the large-scale circular wave would be caused by the acoustic wave generated from the propagating Rayleigh wave. Related to the first wave, anomalous ionospheric echoes were also observed by four ionosonde stations in Japan (Maruyama *et al*., 2011). The second peak of the large-scale circular wave had a propagation velocity of 783 m/s, which is comparable with that of the peak of TEC variations after the 2004 Sumatra earthquake (Otsuka *et al*., 2006) and with the sound speed in the ionosphere. The second peak could be caused by an acoustic wave generated from the sea surface at the ionospheric epicenter.

The medium-scale concentric waves (IV) with a propagation velocity of 138–423 m/s appeared about 300 km away from the ionospheric epicenter and propagated for more than 1,000 km beyond the region of GPS-TEC observations as seen in Figs. 2(g–h). Figure 3 shows that the wavelength and the propagation velocity of these medium-scale waves tended to decrease with time. This characteristic is consistent with the result of numerical simulations with a time-dependent, two-dimensional, nonlinear, non-hydrostatic, compressible and neutral numerical model (Matsumura *et al*., 2011). According to these characteristics, Matsumura *et al*. (2011) suggested that these medium-scale waves correspond to gravity modes of the coseismic atmospheric waves.

The amplitude of the concentric waves was not uniform and depended on an azimuth of their propagation direction as shown in Fig. 2. TEC variations propagating to azimuth between north and west tended to have much larger amplitudes. This directivity regarding the amplitude of the TEC variations is not consistent with those reported by previous papers on TEC variations following earthquakes (e.g., Heki and Ping, 2005; Otsuka *et al*., 2006). Otsuka *et al*. (2006) reported that equatorward-propagating TEC variations had a larger amplitude than poleward-propagating TEC variations. They suggested that the directivity in TEC variations could be caused by the directivity in the response of the plasma density variation to the neutral motion of acoustic waves in oblique geomagnetic field lines, assuming acoustic waves propagate uniformly to all azimuths from a point source. However, this scenario cannot account for the current event. We can speculate that the assumption may not be valid and that northwestward-propagating acoustic waves might have a larger amplitude than waves propagating in other directions.

The circular or concentric structures of the large- and medium-scale waves indicate that these ionospheric disturbances had a point source. The center of these structures, the ionospheric epicenter, is located around 37.5°N of latitude and 144.0°E of longitude, about 170 km from the epicenter in the southeast direction. As discussed previously, atmospheric waves could be launched by the vertical displacement of air above the sea surface. The ionospheric epicenter was closer to the Japan trench than the epicenter and consistent with estimated areas of the tsunami source (e.g., Fujii *et al*., 2011). According to the prompt report of the tsunami in this event by JWA (Japan Weather Association,

2011), the first tsunami strike of the Pacific coast near the epicenter was 10–20 minutes after the earthquake onset. The high-resolution wide-coverage ionospheric observations using a GPS receiver network detected the initial TEC disturbances near the off-coast epicenter about seven minutes after the earthquake onset. The realtime GPS-TEC observations could have a potential to strongly support the current tsunami monitoring system based on tsunami and tide monitors near the coast.

Acknowledgments. GPS data of GEONET were provided by the Geospatial Information Authority of Japan. This study was partially supported by the Grant-in-Aid for Young Scientists (B) (22740326).

References

Artru, J., V. Ducic, H. Kanamori, P. Lognonné, and M. Murakami, Ionospheric detection of gravity waves induced by tsunamis, *Geophys. J. Int.*, **160**, 840–848, 2005.

Chen, C. H., A. Saito, C. H. Lin, J. Y. Liu, H. F. Tsai, T. Tsugawa, Y. Otsuka, M. Nishioka, and M. Matsumura, Long-distance propagation of ionospheric disturbance generated by the 2011 off the Pacific coast of Tohoku Earthquake, *Earth Planets Space*, **63**, this issue, 881–884, 2011.

Davies, K. and D. M. Baker, Ionospheric effects observed around the time of the Alaskan earthquake of March 28, 1964, *J. Geophys. Res.*, **70**, 2251–2253, 1965.

Ducic, V., J. Artru, and P. Lognonné, Ionospheric remote sensing of the Denali Earthquake Rayleigh surface waves, *Geophys. Res. Lett.*, **30**(18), 1951, doi:10.1029/2003GL017812, 2003.

Fujii, Y., K. Satake, S. Sakai, M. Shinohara, and T. Kanazawa, Tsunami source of the 2011 off the Pacific coast of Tohoku Earthquake, *Earth Planets Space*, **63**, this issue, 815–820, 2011.

Heki, K. and J. S. Ping, Directivity and apparent velocity of the coseismic ionospheric disturbances observed with a dense GPS array, *Earth Planet. Sci. Lett.*, **236**, 845–855, 2005.

Japan Weather Association, http://www.jwa.or.jp/, 2011.

Liu, J. Y., H. F. Tsai, C. H. Lin, M. Kamogawa, Y. I. Chen, C. H. Lin, B. S. Huang, S. B. Yu, and Y. H. Yeh, Coseismic ionospheric disturbances triggered by the Chi-Chi earthquake, *J. Geophys. Res.*, **115**, A08303, doi:10.1029/2009JA014943, 2010.

Maruyama, T., T. Tsugawa, H. Kato, A. Saito, Y. Otsuka, and M. Nishioka, Ionospheric multiple stratifications and irregularities induced by the 2011 off the Pacific coast of Tohoku Earthquake, *Earth Planets Space*, **63**, this issue, 869–873, 2011.

Matsumura, M., A. Saito, T. Iyemori, H. Shinagawa, T. Tsugawa, Y. Otsuka, M. Nishioka, and C. H. Chen, Numerical simulations of atmospheric waves excited by the 2011 off the Pacific coast of Tohoku Earthquake, *Earth Planets Space*, **63**, this issue, 885–889, 2011.

Nishioka, M., Y. Otsuka, and K. Shiokawa, GPS total electron content disturbances induced by the 2010 Chile Earthquake, *J. Geophys. Res.*, 2011 (submitted).

Oliver, J., A summary of observed seismic surface wave dispersion, *Bull. Seismol. Soc. Am.*, **52**, 81–86, 1962.

Otsuka, Y., T. Ogawa, A. Saito, T. Tsugawa, S. Fukao, and S. Miyazaki, A new technique for mapping of total electron content using GPS network in Japan, *Earth Planets Space*, **54**, 63–70, 2002.

Otsuka, Y., N. Kotake, T. Tsugawa, K. Shiokawa, T. Ogawa, Effendy, S. Saito, M. Kawamura, T. Maruyama, N. Hemmakorn, and T. Komolmis, GPS detection of total electron content variations over Indonesia and Thailand following the 26 December 2004 earthquake, *Earth Planets Space*, **58**, 159–165, 2006.

Saito, A., S. Fukao, and S. Miyazaki, High resolution mapping of TEC perturbations with the GSI GPS network over Japan, *Geophys. Res. Lett.*, **25**, 3079–3082, 1998.

Saito, A., T. Tsugawa, Y. Otsuka, M. Nishioka, T. Iyemori, M. Matsumura, S. Saito, C. H. Chen, Y. Goi, and N. Choosakul, Acoustic resonance and plasma depletion detected by GPS total electron content observation after the 2011 off the Pacific coast of Tohoku Earthquake, *Earth Planets Space*, **63**, this issue, 863–867, 2011.

U.S. Geological Survey, http://earthquake.usgs.gov/, 2011.

T. Tsugawa (e-mail: tsugawa@nict.go.jp), A. Saito, Y. Otsuka, M. Nishioka, T. Maruyama, H. Kato, T. Nagatsuma, and K. T. Murata